




ORIGINAL ARTICLE

Multomics and single-cell sequencings reveal the specific biological characteristics of low Ki-67 triple-negative breast cancer

Boyue Han^{1,2,3}  | Xiangchen Han^{1,2,3} | Hong Luo³ | Javaria Nasir^{1,2} |
Chao Chen^{1,2} | Zhiming Shao^{1,2,3} | Hong Ling^{1,2}  | Xin Hu^{1,2,3} 

¹Key Laboratory of Breast Cancer in Shanghai, Department of Breast Surgery, Fudan University Shanghai Cancer Center, Shanghai, China

²Department of Oncology, Shanghai Medical College, Fudan University, Shanghai, China

³Precision Cancer Medical Center, Fudan University Shanghai Cancer Center, Shanghai, China

Correspondence

Hong Ling, Key Laboratory of Breast Cancer in Shanghai, Department of Breast Surgery, Fudan University Shanghai Cancer Center, 270 Dong-An Rd, Shanghai 200032, China.
Email: linghong98@aliyun.com

Xin Hu, Precision Cancer Medical Center, Fudan University Shanghai Cancer Center, 270 Dong-An Rd, Shanghai 200032, China.
Email: xinhufd@163.com

Funding information

National Natural Science Foundation of China, Grant/Award Numbers: 81872137, 82072917, 82272957; Shanghai Science and Technology Innovation Action Plan, Grant/Award Number: 22DZ2204400

Abstract

Background: Triple-negative breast cancer (TNBC) displays high heterogeneity. The majority of TNBC cases are characterized by high Ki-67 expression. TNBC with low Ki-67 expression accounts for only a small fraction of cases and has been relatively less studied.

Methods: This study analyzed a large single-center multomics TNBC data set, combined with a single-cell data set. The clinical, genomic, and metabolic characteristics of patients with low Ki-67 TNBC were analyzed.

Results: The clinical and pathological characteristics were analyzed in 2217 TNBC patients. Low Ki-67 TNBC was associated with a higher patient age at diagnosis, a lower proportion of invasive ductal carcinoma, increased alterations in the PI3K-AKT-mTOR pathway, upregulated lipid metabolism pathways, and enhanced infiltration of M2 macrophages. High Ki-67 TNBC exhibited a higher prevalence of TP53 gene mutations, elevated nucleotide metabolism, and increased infiltration of M1 macrophages.

Conclusions: We identified specific genomic and metabolic characteristics unique to low Ki-67 TNBC, which have implications for the development of precision therapies and patient stratification strategies.

KEYWORDS

genomics, Ki-67 index, metabolic pathways, triple-negative breast cancer

Abbreviations: BLIS, basal-like immune-suppressed; DC, dendritic cell; ER, estrogen receptor; FUSCC, Fudan University Shanghai Cancer Center; GO, Gene Ontology; GSVA, gene set variation analysis; HER-2, human epidermal growth factor receptor 2; HRD, homologous recombination deficiency; IDC, invasive ductal carcinoma; LAR, luminal androgen receptor; LOH, loss of heterozygosity; MIF, macrophage migration inhibitory factor; MPS, metabolic pathway-based subtype; OS, overall survival; PCA, principal component analysis; PR, progesterone receptor; RFS, recurrence-free survival; TNBC, triple-negative breast cancer; TNLP, triple-negative low Ki-67 proliferation; t-SNE, t-distributed stochastic neighbor embedding; WES, whole-exome sequencing.

Boyue Han, Xiangchen Han, and Hong Luo contributed equally to this study and shared the co-first authorship.

This is an open access article under the terms of the [Creative Commons Attribution-NonCommercial](https://creativecommons.org/licenses/by-nc/4.0/) License, which permits use, distribution and reproduction in any medium, provided the original work is properly cited and is not used for commercial purposes.

© 2024 The Author(s). *Cancer Innovation* published by John Wiley & Sons Ltd on behalf of Tsinghua University Press.

1 | INTRODUCTION

Triple-negative breast cancer (TNBC) is a subtype of breast cancer that is characterized by the absence of three receptors: estrogen receptor (ER), progesterone receptor (PR), and human epidermal growth factor receptor 2 (HER-2). TNBC accounts for approximately 15%–20% of all breast cancers [1, 2]. Compared with other subtypes, TNBC tends to exhibit more aggressive behavior [3] and is characterized by a higher proliferation rate and typically larger tumor size [4]. TNBC shows insensitivity to hormone receptor-based endocrine therapy and HER-2-targeted therapy [5]. Consequently, TNBC is associated with a poor prognosis and represents a significant threat to women's health [6].

Ki-67 is a nonhistone nuclear protein that is closely associated with cell proliferation activity. Ki-67 is present throughout all phases of the cell cycle except G0 and its expression dynamically changes. Ki-67 levels are relatively low in the G1 and S phases of mitosis, peak in the premitotic phase, and undergo a sharp decline during the postmitotic phase [7]. Elevated Ki-67 expression indicates rapid cell proliferation and increased invasiveness and is a significant indicator of poor prognosis [8, 9]. In clinical pathology, Ki-67 is commonly used as a proliferation marker to assess the invasiveness of breast cancer [10]. Some studies have explored the predictive value of Ki-67 for the efficacy of adjuvant chemotherapy in breast cancer, but the results remain controversial [11]. Criscitiello et al. [12] reported that Ki-67 expression could identify patients benefiting from adjuvant chemotherapy in luminal-B and lymph node-positive breast cancers. Andre et al. [13] reported no evidence supporting the predictive value of Ki-67 staining for the effectiveness of adjuvant chemotherapy.

TNBC displays high heterogeneity. TNBC predominantly consists of invasive ductal carcinoma (IDC), but it also includes less aggressive tumor types, such as mucinous carcinoma, metaplastic carcinoma, secretory carcinoma, and adenoid cystic carcinoma [14, 15]. TNBC often exhibits high expression of the Ki-67 proliferation index [16, 17]. Srivastava et al. [18] reported that more than three-quarters of TNBC patients had Ki-67 expression levels above 50%. TNBC with low Ki-67 expression accounts for only a small fraction of cases and has been relatively less studied. One study conducted by Srivastava et al. [18] demonstrated that triple-negative low Ki-67 proliferation (TNLP) tumors are characterized by a predominance of low to intermediate-grade apocrine tumors. Compared with TNBC patients with high Ki-67 expression, TNLP patients tend to be older, have smaller tumor sizes at the time of diagnosis, and present with lower tumor grades [18]. These findings suggest that low

Ki-67 TNBC might represent distinctive disease entities. However, the biological characteristics of low Ki-67 TNBC remain unclear.

In this study, we conducted a comprehensive analysis of multiomics data from Fudan University Shanghai Cancer Center (FUSCC) to elucidate the clinicopathological features, metabolic pathway characteristics, and immune microenvironment of low Ki-67 TNBC. The aim of this study was to investigate the distinctive biological behaviors of and potential therapeutic strategies for low Ki-67 TNBC.

2 | MATERIALS AND METHODS

2.1 | Study cohorts

This study included female TNBC patients from FUSCC. The inclusion criteria were a diagnosis of breast cancer at our center between 2006 and 2016, with pathological confirmation of ER-negative, PR-negative, and HER-2-negative status. The exclusion criteria were bilateral breast cancer; ductal or lobular atypical hyperplasia, sarcomas, or phyllodes tumors; and missing Ki-67 status (Figure 1). Comprehensive clinical pathology and survival data were available for 2217 patients, RNA-seq data were available for 350 patients, and whole-exome sequencing (WES) data were available for 279 patients. All patients provided informed consent for the appropriate use of their data and tissue [19]. The FUSCC TNBC data set was deposited in the NCBI Gene Expression Omnibus (GSE118527) and Sequence Read Archive (SRP157974). We categorized the patients into two groups using the Ki-67 index obtained from pathological results: the low Ki-67 group ($Ki-67 \leq 20\%$) and the high Ki-67 group ($Ki-67 > 20\%$). The cutoff value of 20% is used in clinical practice at our center.

scRNA-seq data were obtained from external cohorts and are accessible through the European Genome-phenome Archive under the accession number EGAS00001004809 [20]. Using clinical data provided by the public single-cell sequencing database, we classified TNBC patients with low and intermediate Ki-67 levels ($Ki-67 \leq 25\%$) into the Ki-67 low group and TNBC patients with high Ki-67 levels ($>25\%$) into the Ki-67 high group [20].

2.2 | Genome and transcriptome data analyses

To analyze the genomic mutation profiles of different patient groups, the maftools package (v2.14.0) in R was

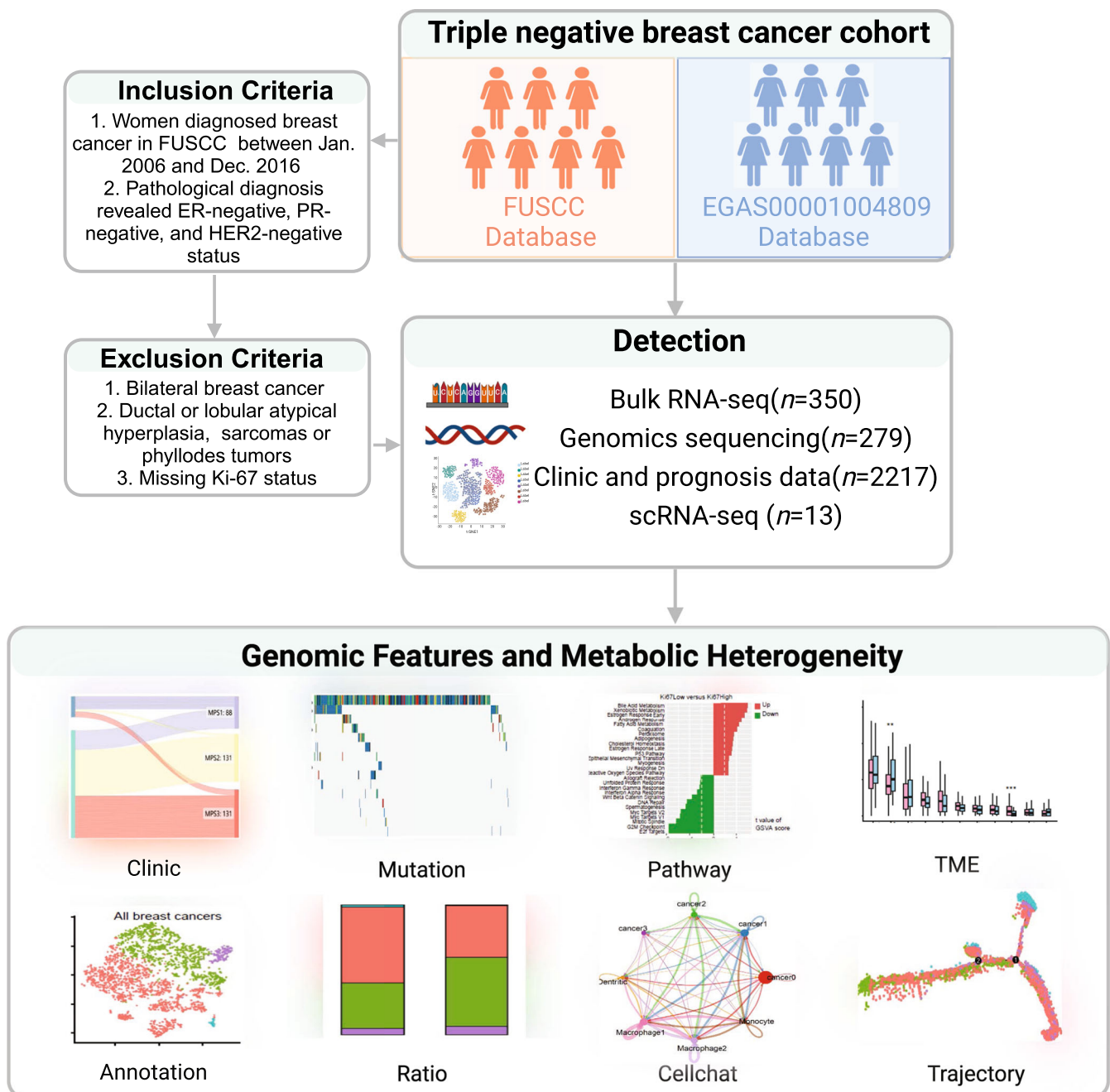


FIGURE 1 A schematic overview of the study workflow. A schematic overview of the analytical workflow and experimental design to explore the genomic features and metabolic heterogeneity of low Ki-67 TNBC is shown. ER, estrogen receptor; FUSCC, Fudan University Shanghai Cancer Center; HER-2, human epidermal growth factor receptor 2; PR, progesterone receptor; TNBC, triple-negative breast cancer.

performed. The definitions and calculations of pathogenic somatic mutations and homologous recombination deficiency (HRD) scores were referenced from the study conducted by Jiang et al. [19]. Somatic mutation pathways were computed on the basis of 10 canonical cancer pathways comprising 335 genes [21]. If recurrent or known driver alterations were detected in one or more genes within a tumor sample, the corresponding cancer pathway was considered to be altered in the tumor sample.

Differential gene expression analyses of RNA-seq data were performed using DESeq. 2 (v1.38.0) in R. Genes with adjusted p -value less than 0.05, after Benjamini–Hochberg false discovery rate correction, were considered differentially expressed genes (DEGs) [22]. Gene set variation analysis (GSVA in R, v1.46.0) was used to calculate the pathway enrichment score for each sample with transcriptomic data using published metabolic pathway gene sets [23, 24]. CIBERSORTx (<https://cibersortx.stanford.edu/>) was used to

examine the abundance of 22 immune cell infiltrates in the tumor microenvironment [25].

2.3 | Cell cultures and reagents

Three human TNBC cell lines (MDA-MB-231, MDA-MB-453, and BT-549) were obtained from American Type Culture Collection. Three mouse TNBC cell lines (4T1, E0771, and AT3) were a gift from Prof. Kang's laboratory (Princeton University). All cell lines were cultured in DMEM (BasalMedia; L110) with 10% fetal bovine serum (Gibco, Thermo Fisher Scientific; 10099141C) and 1% penicillin–streptomycin (BasalMedia; S110B) in a humidified environment consisting of 95% air and 5% CO₂ at 37°C. Cell lines were authenticated by short tandem repeat profiling. Cells were cultured for 48 h for mycoplasma detection and RNA-extraction experiments. All cell lines tested negative for mycoplasma contamination.

2.4 | Immunohistochemical (IHC) staining

Tissue sections from patient samples were provided by the Department of Pathology at FUSCC. For the breast orthotopic tumor implantation experiment, 5×10^5 E0771 cells were injected into the mammary fat pad of 6-week-old female C57BL/6J mice, and 5×10^5 4T1 cells were injected into the mammary fat pad of 6-week-old female BALB/c mice. After 4 weeks, the mice were euthanized, and the orthotopic tumors were excised, sectioned, and prepared for subsequent immunohistochemistry experiments. The sections were heated in an oven at 70°C for 1 h and then dewaxed in xylene. The samples were hydrated using a series of alcohol solutions (100%, 90%, and 70%), followed by antigen retrieval in citrate buffer (pH 6.0) at 95°C for 20 min. The sections were incubated with antibodies at 37°C for 1 to 2 h (anti-fatty acid synthase [FASN] [1:1000, ab128870; Abcam]; anti-Ki-67 [1:1000, ab279653; Abcam]). The nuclei were counterstained with hematoxylin for approximately 10 s.

2.5 | RNA extraction and qRT-PCR

Total RNA was extracted using TRIzol reagent (Invitrogen, Thermo Fisher Scientific; 15596018CN) and then reverse-transcribed into cDNA using HiScript II Q Select RT SuperMix for qPCR (Vazyme; R233-01). The qPCR primers were obtained from PrimerBank (<https://pga.mgh.harvard.edu/primerbank/>) (Supporting Information S2: Table S1). AceQ qPCR SYBR Green Master Mix

(Vazyme; Q111-03) was used for qRT-PCR, and GAPDH mRNA served as the internal control for normalization. All experiments were performed following the manufacturer's recommended protocols.

2.6 | Single-cell RNA-seq data analysis

Single-cell RNA-seq data were mainly analyzed using the Seurat package (v4.3.0). The raw unique multiplex index counts were normalized, and the FindVariableFeatures function was used to detect variable genes. Principal component analysis (PCA) was conducted using the variable genes. For clustering, the FindClusters function was used, implementing a PCA-based shared nearest neighbor approach with a resolution of 0.5 on the first 12 principal components. We performed t-distributed stochastic neighbor embedding (t-SNE) for dimensionality reduction to obtain a two-dimensional representation of cell states. The FindAllMarkers function was used to identify marker genes, and cell annotation was based on these marker genes. EnrichGO function was used for Gene Ontology (GO) pathway enrichment analysis. Monocle (v2.26.0) package was used for cell pseudo-time analysis, and CellChat (v1.6.0) package was used for cell-cell communication analysis.

2.7 | Statistical analyses

Continuous and ordered categorical variables were compared using the Student's *t*-test, Mann–Whitney–Wilcoxon test, and Kruskal–Wallis test. For the comparison of unordered categorical variables, the Pearson chi-square test or Fisher's exact test was used. Survival curves were generated using the Kaplan–Meier method, and the log-rank test was applied to compare recurrence-free survival (RFS) and overall survival (OS) outcomes. All *p*-values were two-sided, and a *p*-value of less than 0.05 was considered statistically significant. R software (versions 4.2.0, www.R-project.org/) and GraphPad Prism software (version 9.0.0, www.graphpad.com) were used for statistical analysis and graph plotting.

3 | RESULTS

3.1 | The study design and cohorts

The study design is shown in Figure 1. We integrated multiomics data of TNBC from FUSCC and single-cell sequencing data from Bassez and colleagues [19, 20] for analysis. The cohort of 2217 TNBC patients treated at our

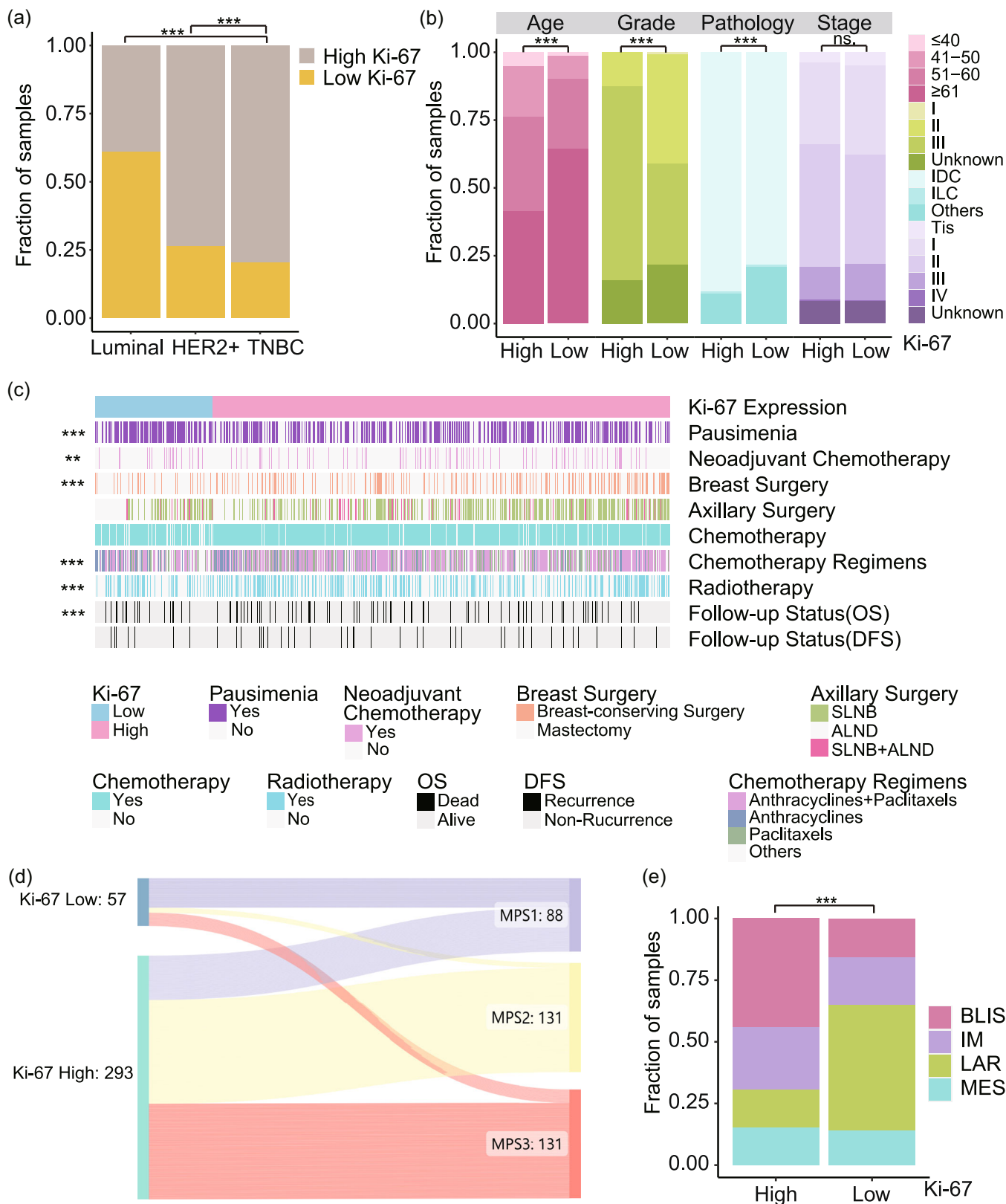


FIGURE 2 (See caption on next page).

center with clinical prognosis data was used for analyzing the clinical prognostic features of low Ki-67 TNBC. RNA-seq data from 350 TNBC cases were used for analyzing DEGs, metabolic pathways, and the immune microenvironment. The WES data of 279 TNBC patients were used for elucidating somatic mutation characteristics. The scRNA-seq data included 13 cases, comprising 8172 tumor cells and 3177 myeloid cells, which were used for cell annotation, cell chat, and evolutionary trajectory analysis.

3.2 | Clinical and prognosis features of low Ki-67 TNBC

The 2217 TNBC patient cohorts indicated that compared with luminal and HER-2 overexpression breast cancer, TNBC had a higher proportion of patients with high Ki-67 expression (TNBC vs. luminal, 79.5% vs. 38.9%, $p < 0.0001$; TNBC vs. HER-2 overexpression, 79.5% vs. 73.6%, $p < 0.001$) (Figure 2a). Most TNBC tumors showed high Ki-67 expression, and only 20.5% of TNBC tumors exhibited low Ki-67 expression. Low Ki-67 TNBC was characterized by an older age at diagnosis (age > 60 years: 64.3% in Ki-67 Low vs. 41.5% in Ki-67 High, $p < 0.001$), lower tumor grade (grade 3: 37.4% in Ki-67 Low vs. 71.6% in Ki-67 High, $p < 0.001$), and a lower prevalence of the IDC histological type (78.4% in Ki-67 Low vs. 88.1% in Ki-67 High, $p < 0.001$). There was no difference in tumor stage between the low Ki-67 and high Ki-67 groups ($p = 0.493$, Figure 2b). The treatment strategies and survival outcomes between low Ki-67 and high Ki-67 TNBC groups are shown in Figure 2c. TNBC with low Ki-67 expression displayed better RFS (5-year RFS: 88.7% in Ki-67 Low TNBC vs. 82.8% in Ki-67 High TNBC, $p < 0.001$) and OS (5-year OS: 93.7% in Ki-67 Low TNBC vs. 90.7% in Ki-67 High TNBC, $p < 0.001$) (Supporting Information S1: Figures S1 and S2).

Previous studies classified TNBC into different subtypes on the basis of gene expression or metabolic pathway features [19, 24]. We next investigated the distribution of molecular subtypes in TNBC with high and low Ki-67 expression. The results revealed that low Ki-67 TNBC was mainly composed of the metabolic pathway-based subtype

1 (MPS1) subtype (61.4%), which is characterized by upregulated lipid metabolism. In contrast, high Ki-67 TNBC was predominantly composed of the glycolytic subtype MPS2 (44.7%) and the mixed subtype MPS3 (44.7%) ($p < 0.001$, Figure 2d). We determined the Fudan transcriptome-based TNBC subtypes for each sample and investigated their distributions in the high and low Ki-67 groups. The low Ki-67 group primarily contained the luminal androgen receptor (LAR) subtype (50.9% in Ki-67 Low vs. 15.4% in Ki-67 High, $p < 0.001$), while the high Ki-67 group had a larger proportion of the basal-like immune-suppressed (BLIS) subtype (50.9% in Ki-67 High vs. 15.4% in Ki-67 Low, $p < 0.001$) (Figure 2e).

3.3 | Mutation profile of low Ki-67 TNBC

Genomic alterations contribute to the high heterogeneity of malignant tumors and exploring these mutations can help identify valuable biomarkers for precise cancer therapy. Figure 3a shows the landscape of the top 15 somatic mutations in TNBC, and the findings revealed significant differences between low Ki-67 TNBC and high Ki-67 TNBC. Low Ki-67 TNBC had a higher frequency of AKT1 gene mutations (low Ki-67 vs. high Ki-67: 11% vs. 2%, $p = 0.015$), while high Ki-67 TNBC exhibited a higher proportion of TP53 gene mutations (high Ki-67 vs. low Ki-67: 79% vs. 47%, $p < 0.001$) (Figure 3a).

To gain a more comprehensive understanding of the mutation profile, we conducted an analysis of mutational profiles based on pathways. Low Ki-67 TNBC had more somatic mutations in the PI3K-AKT-mTOR signaling pathway (low Ki-67 vs. high Ki-67: 50% vs 31%, $p = 0.025$) and RTK-RAS signaling pathway (low Ki-67 vs. high Ki-67: 29% vs 26%, $p = 0.032$), while high Ki-67 TNBC exhibited a higher proportion of mutations in the TP53 signaling pathway (high Ki-67 vs. low Ki-67: 80% vs. 47%, $p < 0.001$) (Figure 3b). We investigated the significant co-occurring and mutually exclusive alterations within the different pathways. We observed a significant mutually exclusive pattern unique to the high Ki-67 group involving the TP53 and TGF- β signaling pathways

FIGURE 2 Clinical, pathological, and therapeutic characteristics of the FUSCC TNBC cohort. (a) Bar plots showing the proportion of low and high Ki-67 expression in different subtypes of breast cancer. (b) Bar plots showing the distribution of age, grade, pathology type, and stage in the low and high Ki-67 groups. (c) Associations of Ki-67 expression with menstrual status, treatment strategies, and prognosis in TNBC. (d) Sankey diagram illustrating the metabolic subtypes in the low and high Ki-67 groups. (e) Bar plots illustrating the Fudan transcriptome-based TNBC subtypes in the low and high Ki-67 groups. FUSCC, Fudan University Shanghai Cancer Center; IDC, invasive ductal carcinoma; ILC, invasive lobular carcinoma; Others, other cancers including mucinous carcinoma, metaplastic carcinoma, secretory carcinoma, and adenoid cystic carcinoma; Tis, carcinoma in situ; TNBC, triple-negative breast cancer. ** $p < 0.01$; ** $p < 0.001$; n.s., not significant.

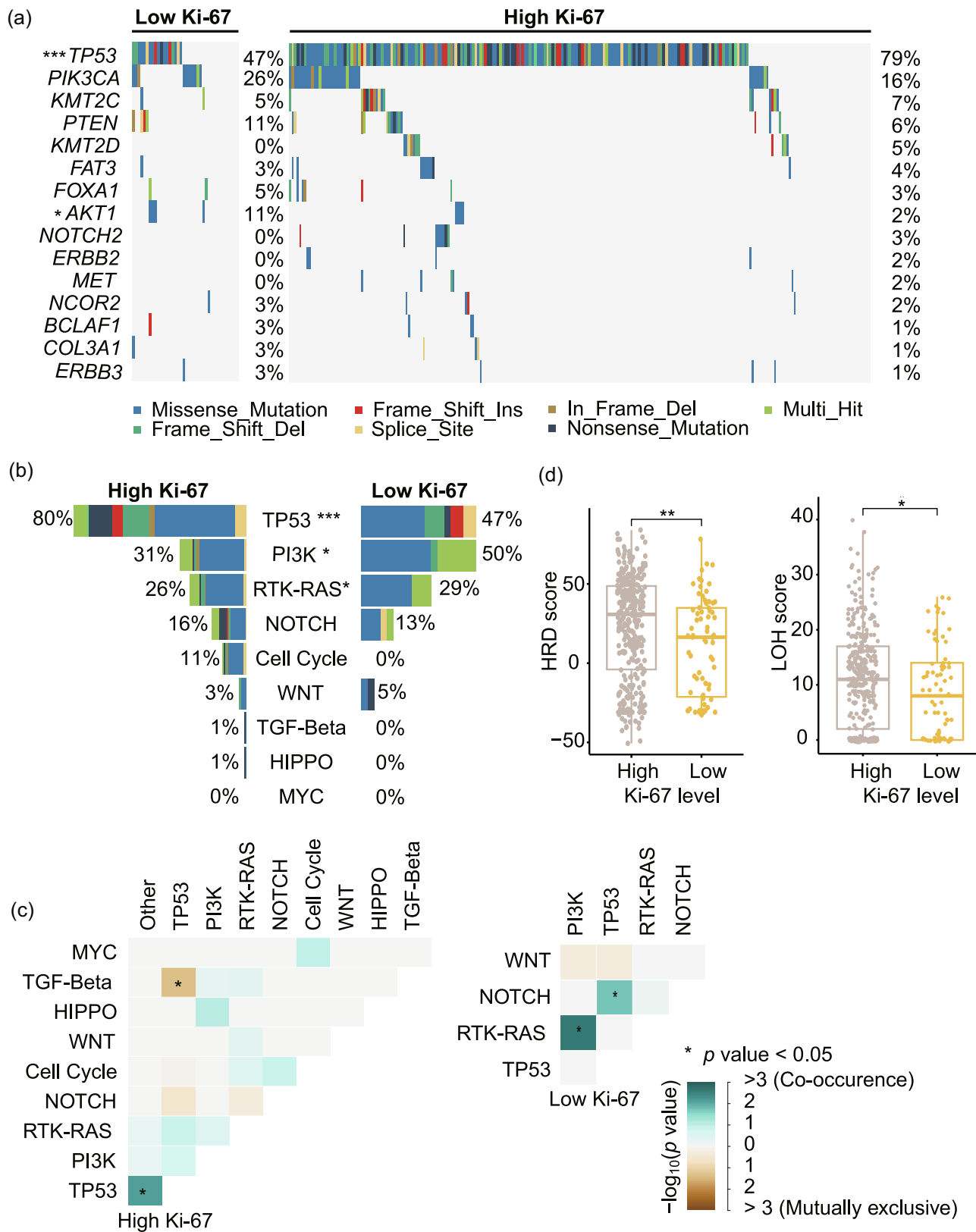


FIGURE 3 Genomic landscape and featured oncogenic pathways in low Ki-67 TNBC. (a) Genomic landscape of somatic mutations in the low and high Ki-67 groups. (b) Comparison of genomic alterations in nine oncogenic pathways between the low and high Ki-67 groups in the FUSCC cohort. (c) Significant mutual exclusivity (brownish yellow) and co-occurrence (dark green) of gene mutations in pathways between the low and high Ki-67 groups. (d) Box plots showing the homologous recombination deficiency (HRD) and loss of heterozygosity (LOH) scores. FUSCC, Fudan University Shanghai Cancer Center; TNBC, triple-negative breast cancer. * $p < 0.05$; ** $p < 0.01$; *** $p < 0.001$.

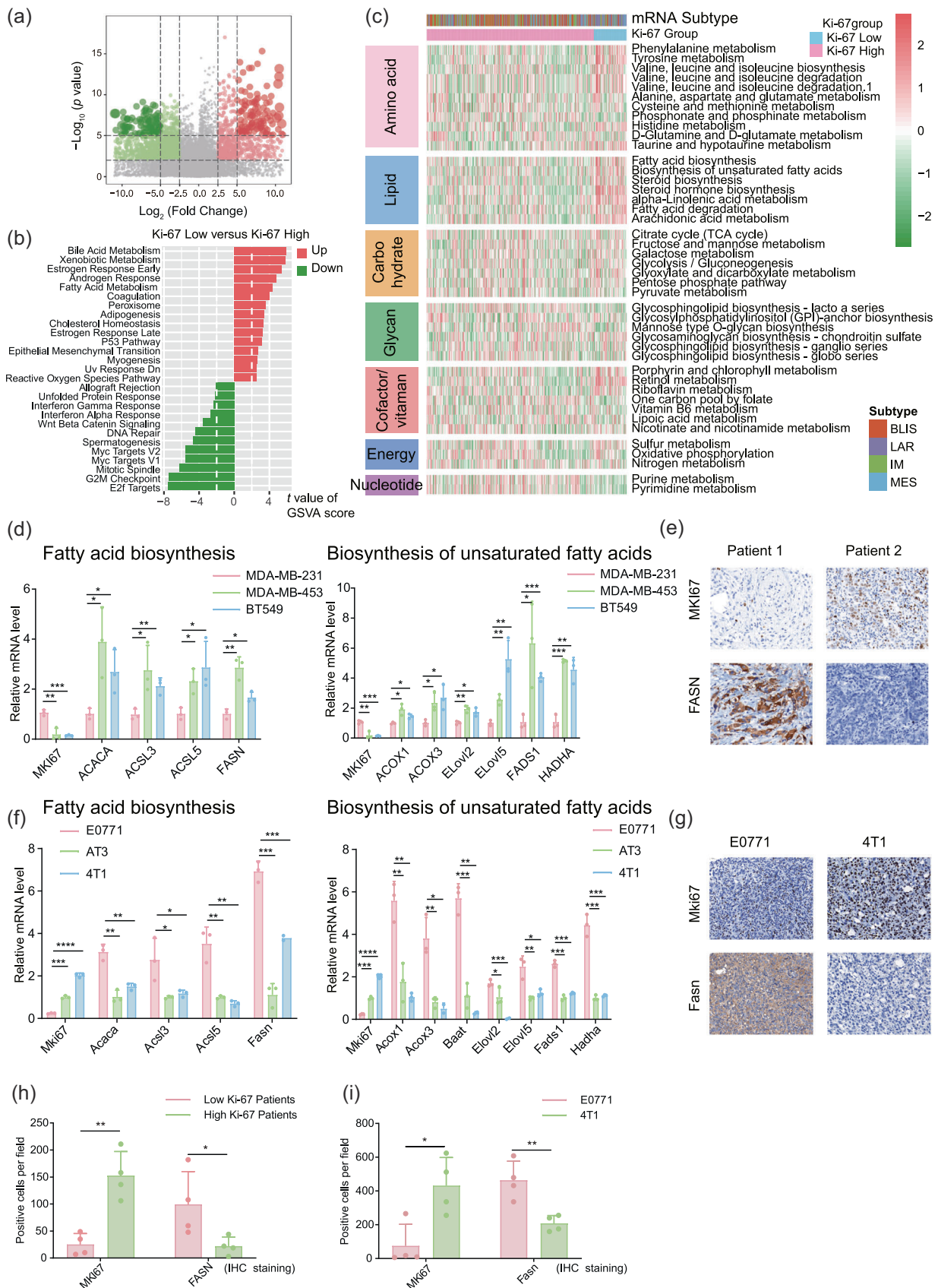


FIGURE 4 (See caption on next page).

($p = 0.041$) (Figure 3c). Significant co-occurring alterations were exclusively found in the low Ki-67 group in the TP53 and NOTCH signaling pathways ($p = 0.047$) and the PI3K-AKT-mTOR and RTK-RAS signaling pathways ($p = 0.011$) (Figure 3c). We further explored genomic stability and observed that the low Ki-67 TNBC group exhibited lower HRD scores ($p = 0.0043$) and lower loss of heterozygosity scores ($p = 0.0442$) compared with the high Ki-67 group (Figure 3d).

3.4 | Dysregulated metabolic pathways and targetable metabolic genes in the low Ki-67 group

We performed differential expression analysis of the low and high Ki-67 groups. The volcano plot displayed 1425 upregulated genes and 2266 downregulated genes in the low Ki-67 group, with a threshold of $|\log_2FC| > 2.5$ and adjusted $p < 0.05$ (Figure 4a). These results indicated significant differences in gene expression between the two groups and suggest potential candidate genes associated with the Ki-67 index in TNBC. We next used hallmark gene sets from the Molecular Signatures Database to analyze the pathway alterations [26]. We observed a marked upregulation of various metabolic pathways in the low Ki-67 group, including fatty acid metabolism, cholesterol homeostasis, and adipogenesis (Figure 4b). In the high Ki-67 group, there was an upregulation of cell cycle signaling pathways, including the mitotic spindle and G2M checkpoint (Figure 4b).

To uncover the metabolic heterogeneity of low Ki-67 TNBC, we used GSVA to estimate the enrichment scores of metabolic pathways [23]. Consistent with the GSVA results, the low Ki-67 group exhibited upregulation of lipid metabolism, while the high Ki-67 group showed upregulation of nucleotide metabolism (Figure 4c, Supporting Information S1: Figure S3a). The RNA-seq results

revealed that metabolic genes in the fatty acid biosynthesis and biosynthesis of unsaturated fatty acids pathways were upregulated in the low Ki-67 group (Supporting Information S1: Figure S3b,c).

We further examined the upregulation of metabolic pathways in the low Ki-67 group through experiments. We selected three human TNBC cell lines for analysis and observed that the MDA-MB-231 cell line had high Ki-67 expression, while the MDA-MB-453 and BT-549 cell lines had relatively low Ki-67 expression. The cell lines with low Ki-67 expression exhibited increased expression of metabolic genes involved in fatty acid biosynthesis and unsaturated fatty acid biosynthesis pathways (Figure 4d). The same trend was observed in three murine TNBC cell lines (Figure 4f). Using TNBC patient tissue sections from our center, we performed IHC staining for Ki-67 and FASN. The results indicated that patients with low Ki-67 expression had high FASN expression (Figure 4e,h). We observed the same trend in tissue sections from orthotopic breast tumor models in mice (Figure 4g,i). These findings were consistent with our bioinformatics analysis, suggesting that low Ki-67 TNBC exhibited upregulated lipid metabolism pathways.

3.5 | The tumor microenvironment and heterogeneity of myeloid cells

To explore the features of the tumor immune microenvironment in the low Ki-67 group, we used the CIBERSORT method to calculate the abundance of 22 immune cell types [27]. The results revealed significant differences in the abundance of three immune cell types between the low Ki-67 and high Ki-67 groups, including macrophage 2 (M2) ($p = 0.0054$), memory B cells ($p = 0.0006$), and activated dendritic cells (DCs) ($p = 0.021$) (Figure 5a, Supporting Information S1: Figure S4a).

FIGURE 4 Dysregulated metabolic pathways and targetable metabolic genes in the low Ki-67 group. (a) Volcano plot displaying the differentially expressed genes between the low and high Ki-67 groups. Genes upregulated in the low Ki-67 group are shown in red, while downregulated genes are shown in green. (b) Bar plot illustrating pathway analysis enriched with differentially expressed genes. The t value represents the difference in average enrichment scores between two groups in GSVA. A larger absolute t value indicates a significant difference in pathway activity between the two groups. (c) Heatmap illustrating the GSVA of the expression levels of metabolic pathways in low and high Ki-67 groups. (d) Bar plot showing the differentially expressed genes in the fatty acid biosynthesis and unsaturated fatty acid biosynthesis pathways between Ki-67 low and high groups in three human TNBC cell lines. (e) Representative images of immunohistochemical (IHC) staining for Ki-67 and FASN in TNBC patient tissue sections. (f) Bar plot showing the differentially expressed genes in the fatty acid biosynthesis and unsaturated fatty acid biosynthesis pathways between Ki-67 low and high groups in three murine TNBC cell lines. (g) Representative images of IHC staining for Ki-67 and FASN in tissue sections from orthotopic breast tumor mouse models. (h) Ki-67 and FASN expression quantified by IHC in TNBC patient tissue sections. (i) Ki-67 and FASN expression quantified by IHC in tissue sections from orthotopic breast tumor mouse models. FASN, fatty acid synthase; GSVA, gene set variation analysis; TNBC, triple-negative breast cancer. * $p < 0.05$; ** $p < 0.01$; *** $p < 0.001$.

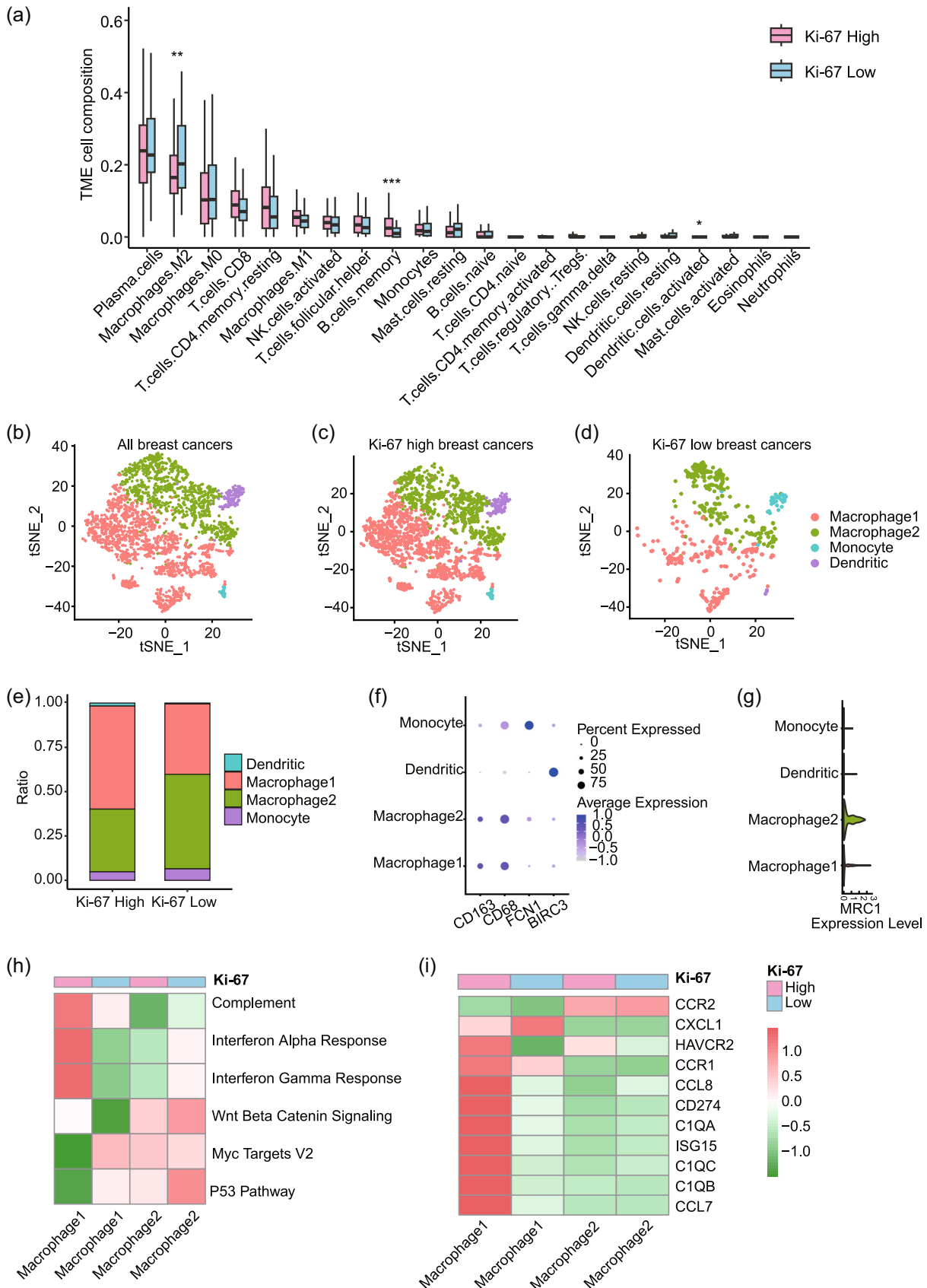


FIGURE 5 (See caption on next page).

scRNA-seq data were used to comprehensively assess the expression profile of myeloid cells. After quality filtering, a total of 3177 myeloid cells were analyzed. Using t-SNE, we identified four clusters: Macrophage1, Macrophage2, Monocyte, and DCs (Figure 5b–d). Figure 5f,g depict the clustering markers, facilitating the linkage of clusters to specific cell types, including M1-like macrophages (CD163, CD68, MRC–), M2-like macrophages (CD163, CD68, MRC+), monocyte (FCN1), and DCs (BIRC3) (Figure 5f–g, Supporting Information S1: Figure S4c–f).

M1-like macrophages (antitumor) and M2-like macrophages (pro-tumor) are two major macrophage subtypes [28]. Our results revealed an increased prevalence of M2-like macrophages in the low Ki-67 group, indicating the presence of an immunosuppressive microenvironment (Figure 5e). Pathway analysis of macrophages revealed that in the high Ki-67 group, M1-like macrophages exhibited upregulation of immune-related signaling pathways, including the complement pathway and interferon alpha/gamma response. Conversely, in the low Ki-67 group, M2-like macrophages showed upregulation of protumorigenic signaling pathways, such as the Wnt beta-catenin signaling pathway (Figure 5h). Gene analysis further revealed that M1-like macrophages in the high Ki-67 group exhibited upregulation of immune activation-related genes such as C1QA, ISG15, C1QC, and C1QB genes (Figure 5i).

In summary, our results suggested that the low Ki-67 group was predominantly infiltrated by M2-like macrophages, which promote tumor progression, while the high Ki-67 group was mainly infiltrated by M1-like macrophages, which exhibit an immune-activating anti-tumor effect.

3.6 | Tumor cell heterogeneity and interactions between tumor cells and myeloid cells

To investigate the heterogeneity of tumor cells in TNBC, we identified four clusters of tumor cells in TNBC through t-SNE analysis; each cluster exhibited distinct transcriptomic signatures (Figure 6a,b, Supporting

Information S1: Figure S5a). Cluster 1 was the major cell population in the low Ki-67 group, while clusters 2 and 3 were specifically enriched in the high Ki-67 group (Figure 6c). GO analyses revealed that cluster 0 was mainly enriched in extracellular matrix structural constituent; cluster 1 showed enrichment in oxidative phosphorylation and aerobic respiration; cluster 2 was primarily enriched in extracellular matrix structural constituent; and cluster 3 exhibited enrichment in pyridine nucleotide metabolic process and nicotinamide nucleotide metabolic processes (Figure 6d–g). These results suggested differential intrinsic biological characteristics in tumor cells between low and high Ki-67 groups, with upregulated lipid metabolism in low Ki-67 cells and increased proliferation and nucleotide metabolism in high Ki-67 cells.

We conducted pseudo-time analysis to investigate the cell lineage trajectory and found that the low Ki-67 tumor cells were in the early stages of cell differentiation (Figure 6h–j). CellChat analysis indicated that tumor cells and macrophages mostly interacted through the macrophage migration inhibitory factor (MIF; CD74 + CD4) receptor–ligand interaction (Figure 6k, Supporting Information S1: Figure S5b,c). Moreover, cluster 1, as the sender, exhibited the most significant impact on M2 macrophages through the MIF signaling pathway (Figure 6l).

4 | DISCUSSION

The findings of this study confirmed that low Ki-67 TNBC exhibited distinct clinical, pathological, and biological characteristics compared with high Ki-67 TNBC, indicating that the two may potentially represent entirely different entities. Low Ki-67 TNBC was characterized by an older patient age at diagnosis, a reduced proportion of IDC, increased alterations in the PI3K-AKT-mTOR pathway, upregulated lipid metabolism pathways, and enhanced infiltration of M2 macrophages. High Ki-67 TNBC exhibited a higher prevalence of TP53 gene mutations, elevated nucleotide metabolism, and increased infiltration of M1 macrophages. Most TNBC cases exhibit high Ki-67 expression, and the most common therapeutic approach is systemic chemotherapy

FIGURE 5 Characteristics of myeloid cells in low Ki-67 TNBC. (a) Bar plot displaying the infiltration abundance of 22 immune cell types in the low and high Ki-67 groups. (b–d) t-SNE display and graph-based clustering of myeloid cells in all TNBC, low Ki-67 TNBC, and high Ki-67 TNBC cases, respectively. (e) Bar graph illustrating the distribution of the indicated t-SNE subsets within the four myeloid cell clusters. (f) Dot plot showing the expression levels of clustering markers for myeloid cells. (g) Violin plots showing the expression levels of MRC1, the clustering marker for M2 macrophages. (h) and (i) Heatmap showing differences in the pathways and genes of interest in M1 and M2 macrophages. TNBC, triple-negative breast cancer; t-SNE, t-distributed stochastic neighbor embedding.

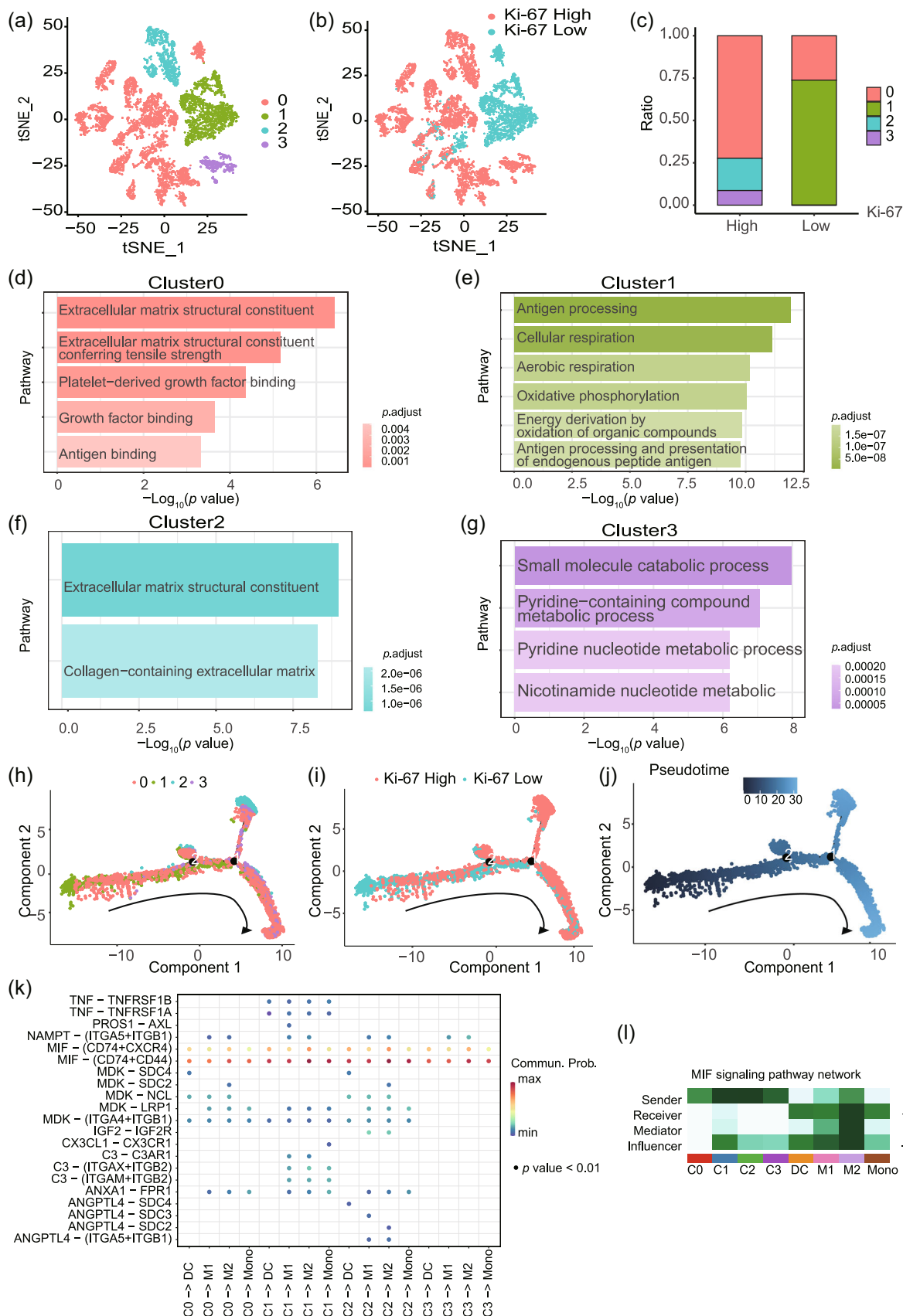


FIGURE 6 (See caption on next page).

[18]. However, there is a subset of TNBC cases with a low Ki-67 proliferation index, which have not been thoroughly investigated. Our study demonstrated that low Ki-67 TNBC typically exhibited lower histological grades and nonclassical histological subtypes, including mucinous carcinoma, metaplastic carcinoma, secretory carcinoma, and adenoid cystic carcinoma. The histological heterogeneity of low Ki-67 TNBC suggests that special attention is needed in the clinical treatment of this particular subtype of TNBC. Previous studies indicated that low Ki-67 TNBC tumors in stage I might not derive significant benefits from chemotherapy [18]. Therefore, clinical practitioners should exercise caution and comprehensive consideration when deciding on the use of chemotherapy and the choice of chemotherapy regimen for low Ki-67 TNBC.

Previous research from our center has classified TNBCs into four transcriptome-based subtypes: (1) LAR, (2) immunomodulatory (IM), (3) BLIS, and (4) mesenchymal-like (MES) [19]. Our study found that low Ki-67 index was predominantly associated with the LAR subtype. This observation was consistent with previous research [29]. The LAR subtype is characterized by elevated expression levels of genes related to the androgen receptor (AR) pathway, and patients with this subtype of TNBC show sensitivity to AR antagonist therapy. AR-positive TNBCs commonly exhibit PIK3CA mutations, and emerging data indicates that combining an AR antagonist with a PI3K inhibitor might yield greater clinical advantages compared with anti-AR therapy alone in AR-positive TNBC cases [30, 31]. This insight could potentially lead to further investigations into targeting AR antagonists for the treatment of low Ki-67 TNBC.

Metabolic reprogramming is one of the distinctive characteristics of TNBC, offering opportunities for prognosis and treatment [32–34]. Our findings indicated that low Ki-67 TNBC was predominantly composed of the MPS1 subtype [24]. The MPS1 subtype is characterized by the upregulation of genes associated with lipid synthesis and metabolism, along with frequent mutations in the PI3K and RTK-RAS pathways [35]. Our analyses of the metabolic and mutation pathways corresponded with these results. Activation of the PI3K pathway in tumor

cells increases the expression of nutrient transporters and enhances lipid synthesis [36]. Furthermore, overexpression of mutant PIK3CA induced a lipid phenotype in nontransformed epithelial cells [37, 38]. These findings underscore the necessity for an in-depth exploration of how the PI3K pathway orchestrates lipid synthesis in TNBC. This may also provide a rationale for the application of lipid synthesis inhibitors in low Ki-67 TNBC.

The analysis of single-cell sequencing data indicated that in low Ki-67 TNBC, the infiltrating macrophages were predominantly of the M2 type. M2 macrophages exhibit anti-inflammatory functions, suggesting that low Ki-67 TNBC possesses an immunosuppressive microenvironment [39]. Additionally, single-cell sequencing data analysis revealed heterogeneity in tumor cells between the Ki-67 low and Ki-67 high groups. The dominant cluster 1 in the Ki-67 low group showed enrichment in oxidative phosphorylation and aerobic respiration, and this was consistent with the bulk-RNA sequencing metabolic pathway analysis results. This cluster primarily interacted with macrophages through the MIF (CD74 + CD4) receptor–ligand interaction, underscoring the significant role of M2 macrophages in Ki-67 low TNBC. Kaneda et al. [40] demonstrated the critical role of PI3K γ in promoting immunosuppressive functions in M2 macrophages within the tumor microenvironment. PI3K γ inhibitors counteract M2 macrophages, thereby rendering tumor cells that were inherently resistant to immune checkpoint inhibitors like PD-1 and CTLA-4 sensitive to immune therapy [41]. In our study, the PI3K pathway mutation frequency in the low Ki-67 TNBC group was 50%, accompanied by an increase in M2 macrophage infiltration. This suggests a potential for the combined application of PI3K γ inhibitors and immune checkpoint inhibitors in the treatment of low Ki-67 TNBC.

A strength of this study is that the study cohort was the largest single-center multiomics cohort of low Ki-67 TNBC patients, enabling the systematic elucidation of the characteristics of low Ki-67 TNBC at the genomic, transcriptomic, and single-cell levels. Our research also establishes a theoretical foundation for the combined therapy involving PI3K pathway inhibitors and

FIGURE 6 Characterization of tumor cells and interactions between tumor cells and myeloid cells. (a) and (b) t-SNE display and graph-based clustering of cancer cells group by subclusters or Ki-67 expression. (c) Bar graph illustrating the distribution of the indicated t-SNE subsets within the four cancer cell clusters. (d–g) GO analysis in different cancer cell subclusters. (h–j) Trajectory of cancer cell differentiation predicted by monocle 2. (k) Bubble plots show significant ligand-receptor pairs between cancer cells and myeloid cells. (l) MIF signaling pathway network between cancer cells and myeloid cells. C0, Cluster 0 of cancer cells; C1, Cluster1 of cancer cells; C2, Cluster2 of cancer cells; C3, Cluster3 of cancer cells; DC, dendritic cell; FUSCC, Fudan University Shanghai Cancer Center; GO, Gene Ontology; M1, Macrophage1; M2, Macrophage2; MIF, macrophage migration inhibitory factor; Mono, monocyte; TNBC, triple-negative breast cancer; t-SNE, t-distributed stochastic neighbor embedding.

immunotherapy for low Ki-67 TNBC. This study also has some limitations. This was a single-center retrospective study, and further validation in cohorts from other centers is required. Prospective clinical trials are needed to explore potential therapeutic strategies for low Ki-67 TNBC.

5 | CONCLUSIONS

The study confirmed that in comparison with high Ki-67 TNBC, low Ki-67 TNBC exhibited distinct clinical, pathological, and biological characteristics, indicating that the two may potentially represent entirely different entities. We identified specific genomic and metabolic characteristics unique to low Ki-67 TNBC, which have implications for the development of precision therapies and patient stratification strategies.

AUTHOR CONTRIBUTIONS

Boyue Han: Conceptualization (equal); data curation (equal); investigation (equal); resources (equal); visualization (equal); writing—original draft (equal); writing—review and editing (equal). **Xiangchen Han:** Conceptualization (equal); data curation (equal); project administration (equal); resources (equal); writing—original draft (equal); writing—review and editing (equal). **Hong Luo:** Formal analysis (equal); investigation (equal); resources (equal); software (equal). **Javaria Nasir:** Data curation (equal); investigation (equal); software (equal). **Chao Chen:** Resources (equal); software (equal); supervision (equal). **Zhiming Shao:** Supervision (equal); validation (equal); writing—review and editing (equal). **Hong Ling:** Investigation (equal); methodology (equal); project administration (equal); resources (equal); supervision (equal). **Xin Hu:** Funding acquisition (equal); project administration (equal); writing—review and editing (equal).

ACKNOWLEDGMENTS

None.

CONFLICT OF INTEREST STATEMENT

The authors declare no conflict of interest.

DATA AVAILABILITY STATEMENT

All data supporting the findings of this study are available from the corresponding author upon reasonable request.

ETHICS STATEMENT

This study did not involve animals. All procedures performed in studies involving human participants were in

accordance with the ethical standards of the institutional and/or national research committee and with the 1964 Helsinki Declaration and its later amendments or comparable ethical standards. This retrospective study was approved by the Ethics Committee Review Board of Fudan University Shanghai Cancer Center (050432).

INFORMED CONSENT

All the patients provided written informed consent for NGS-based genomic testing.

ORCID

Boyue Han  <http://orcid.org/0000-0002-3064-0776>

Hong Ling  <http://orcid.org/0000-0002-9513-3994>

Xin Hu  <http://orcid.org/0000-0002-8160-8362>

REFERENCES

- Metzger-Filho O, Tutt A, de Azambuja E, Saini KS, Viale G, Loi S, et al. Dissecting the heterogeneity of triple-negative breast cancer. *J Clin Oncol.* 2012;30(15):1879–87. <https://doi.org/10.1200/JCO.2011.38.2010>
- Venkitaraman R. Triple-negative/basal-like breast cancer: clinical, pathologic and molecular features. *Expert Rev Anticancer Ther.* 2010;10(2):199–207. <https://doi.org/10.1586/era.09.189>
- Yin WJ, Lu JS, Di GH, Lin YP, Zhou LH, Liu GY, et al. Clinicopathological features of the triple-negative tumors in Chinese breast cancer patients. *Breast Cancer Res Treat.* 2009;115(2):325–33. <https://doi.org/10.1007/s10549-008-0096-0>
- Carey L, Winer E, Viale G, Cameron D, Gianni L. Triple-negative breast cancer: disease entity or title of convenience? *Nat Rev Clin Oncol.* 2010;7(12):683–92. <https://doi.org/10.1038/nrclinonc.2010.154>
- Denkert C, Liedtke C, Tutt A, von Minckwitz G. Molecular alterations in triple-negative breast cancer—the road to new treatment strategies. *The Lancet.* 2017;389(10087):2430–42. [https://doi.org/10.1016/s0140-6736\(16\)32454-0](https://doi.org/10.1016/s0140-6736(16)32454-0)
- Bianchini G, Balko JM, Mayer IA, Sanders ME, Gianni L. Triple-negative breast cancer: challenges and opportunities of a heterogeneous disease. *Nat Rev Clin Oncol.* 2016;13(11):674–90. <https://doi.org/10.1038/nrclinonc.2016.66>
- Scholzen T, Gerdes J. The Ki-67 protein: from the known and the unknown. *J Cell Physiol.* 2000;182(3):311–22. [https://doi.org/10.1002/\(SICI\)1097-4652\(200003\)182:3<311:AID-JCP1>3.0.CO;2-9](https://doi.org/10.1002/(SICI)1097-4652(200003)182:3<311:AID-JCP1>3.0.CO;2-9)
- Denkert C, Budczies J, von Minckwitz G, Wienert S, Loibl S, Klauschen F. Strategies for developing Ki67 as a useful biomarker in breast cancer. *The Breast.* 2015;24(Suppl 2):S67–72. <https://doi.org/10.1016/j.breast.2015.07.017>
- Keam B, Im SA, Lee KH, Han SW, Oh DY, Kim JH, et al. Ki-67 can be used for further classification of triple negative breast cancer into two subtypes with different response and prognosis. *Breast Cancer Res.* 2011;13(2):R22. <https://doi.org/10.1186/bcr2834>
- Wu Q, Ma G, Deng Y, Luo W, Zhao Y, Li W, et al. Prognostic value of ki-67 in patients with resected triple-negative breast cancer: a meta-analysis. *Front Oncol.* 2019;9:1068. <https://doi.org/10.3389/fonc.2019.01068>

11. Ács B, Zámbo V, Vízkeleti L, Szász AM, Madaras L, Szentmártoni G, et al. Ki-67 as a controversial predictive and prognostic marker in breast cancer patients treated with neoadjuvant chemotherapy. *Diagn Pathol.* 2017;12(1):20. <https://doi.org/10.1186/s13000-017-0608-5>
12. Criscitiello C, Disalvatore D, De Laurentiis M, Gelao L, Fumagalli L, Locatelli M, et al. High Ki-67 score is indicative of a greater benefit from adjuvant chemotherapy when added to endocrine therapy in luminal B HER2 negative and node-positive breast cancer. *Breast.* 2014;23(1):69–75. <https://doi.org/10.1016/j.breast.2013.11.007>
13. Andre F, Arnedos M, Goubar A, Ghouadni A, Delaloge S. Ki67—no evidence for its use in node-positive breast cancer. *Nat Rev Clin Oncol.* 2015;12(5):296–301. <https://doi.org/10.1038/nrclinonc.2015.46>
14. Geyer FC, Pareja F, Weigelt B, Rakha E, Ellis IO, Schnitt SJ, et al. The spectrum of triple-negative breast disease. *Am J Pathol.* 2017;187(10):2139–51. <https://doi.org/10.1016/j.ajpath.2017.03.016>
15. Pareja F, Da Cruz Paula A, Gualarte-Mérida R, Vahdatinia M, Li A, Geyer FC, et al. Pleomorphic adenomas and mucoepithelioid carcinomas of the breast are underpinned by fusion genes. *NPJ Breast Cancer.* 2020;6:20. <https://doi.org/10.1038/s41523-020-0164-0>
16. Bhargava R, Striebel J, Beriwal S, Flickinger JC, Onisko A, Ahrendt G, et al. Prevalence, morphologic features and proliferation indices of breast carcinoma molecular classes using immunohistochemical surrogate markers. *Int J Clin Exp Pathol.* 2009;2(5):444–55.
17. Rhee J, Han SW, Oh DY, Kim JH, Im SA, Han W, et al. The clinicopathologic characteristics and prognostic significance of triple-negative breast cancer. *BMC Cancer.* 2008;8:307. <https://doi.org/10.1186/1471-2407-8-307>
18. Srivastava P, Wang T, Clark BZ, Yu J, Fine JL, Villatoro TM, et al. Clinical-pathologic characteristics and response to neoadjuvant chemotherapy in triple-negative low Ki-67 proliferation (TNLP) breast cancers. *NPJ Breast Cancer.* 2022;8(1):51. <https://doi.org/10.1038/s41523-022-00415-z>
19. Jiang YZ, Ma D, Suo C, Shi J, Xue M, Hu X, et al. Genomic and transcriptomic landscape of triple-negative breast cancers: subtypes and treatment strategies. *Cancer Cell.* 2019;35(3):428–40.e5. <https://doi.org/10.1016/j.ccell.2019.02.001>
20. Bassez A, Vos H, Van Dyck L, Floris G, Arijs I, Desmedt C, et al. A single-cell map of intratumoral changes during anti-PD1 treatment of patients with breast cancer. *Nat Med.* 2021;27(5):820–32. <https://doi.org/10.1038/s41591-021-01323-8>
21. Sanchez-Vega F, Mina M, Armenia J, Chatila WK, Luna A, La KC, et al. Oncogenic signaling pathways in the cancer genome atlas. *Cell.* 2018;173(2):321–37.e10. <https://doi.org/10.1016/j.cell.2018.03.035>
22. Love MI, Huber W, Anders S. Moderated estimation of fold change and dispersion for RNA-seq data with DESeq. 2. *Genome Biol.* 2014;15(12):550. <https://doi.org/10.1186/s13059-014-0550-8>
23. Hänzelmann S, Castelo R, Guinney J. GSEA gene set variation analysis for microarray and RNA-seq data. *BMC Bioinformatics.* 2013;14:7. <https://doi.org/10.1186/1471-2105-14-7>
24. Gong Y, Ji P, Yang YS, Xie S, Yu TJ, Xiao Y, et al. Metabolic-pathway-based subtyping of triple-negative breast cancer reveals potential therapeutic targets. *Cell Metab.* 2021;33(1):51–64.e9. <https://doi.org/10.1016/j.cmet.2020.10.012>
25. Newman AM, Steen CB, Liu CL, Gentles AJ, Chaudhuri AA, Scherer F, et al. Determining cell type abundance and expression from bulk tissues with digital cytometry. *Nat Biotechnol.* 2019;37(7):773–82. <https://doi.org/10.1038/s41587-019-0114-2>
26. Liberzon A, Birger C, Thorvaldsdóttir H, Ghandi M, Mesirov JP, Tamayo P. The molecular signatures database hallmark gene set collection. *Cell Systems.* 2015;1(6):417–25. <https://doi.org/10.1016/j.cels.2015.12.004>
27. Chen B, Khodadoust MS, Liu CL, Newman AM, Alizadeh AA. Profiling tumor infiltrating immune cells with CIBERSORT. *Methods Mol Biol.* 2018;1711:243–59. https://doi.org/10.1007/978-1-4939-7493-1_12
28. Mehta AK, Kadel S, Townsend MG, Oliwa M, Guerriero JL. Macrophage biology and mechanisms of immune suppression in breast cancer. *Front Immunol.* 2021;12:643771. <https://doi.org/10.3389/fimmu.2021.643771>
29. Lehmann BD, Jovanović B, Chen X, Estrada MV, Johnson KN, Shyr Y, et al. Refinement of triple-negative breast cancer molecular subtypes: implications for neoadjuvant chemotherapy selection. *PLoS One.* 2016;11(6):e0157368. <https://doi.org/10.1371/journal.pone.0157368>
30. Lehmann BD, Abramson VG, Sanders ME, Mayer EL, Haddad TC, Nanda R, et al. TBCRC 032 IB/II multicenter study: molecular insights to AR antagonist and PI3K inhibitor efficacy in patients with AR⁺ metastatic triple-negative breast cancer. *Clin Cancer Res.* 2020;26(9):2111–23. <https://doi.org/10.1158/1078-0432.CCR-19-2170>
31. Lehmann BD, Bauer JA, Schafer JM, Pendleton CS, Tang L, Johnson KC, et al. PIK3CA mutations in androgen receptor-positive triple negative breast cancer confer sensitivity to the combination of PI3K and androgen receptor inhibitors. *Breast Cancer Res.* 2014;16(4):406. <https://doi.org/10.1186/s13058-014-0406-x>
32. Daemen S, Gemmink A, Brouwers B, Meex RCR, Huntjens PR, Schaart G, et al. Distinct lipid droplet characteristics and distribution unmask the apparent contradiction of the athlete's paradox. *Mol Metab.* 2018;17:71–81. <https://doi.org/10.1016/j.molmet.2018.08.004>
33. Du T, Sikora MJ, Levine KM, Tasdemir N, Riggins RB, Wendell SG, et al. Key regulators of lipid metabolism drive endocrine resistance in invasive lobular breast cancer. *Breast Cancer Res.* 2018;20(1):106. <https://doi.org/10.1186/s13058-018-1041-8>
34. Gaude E, Frezza C. Tissue-specific and convergent metabolic transformation of cancer correlates with metastatic potential and patient survival. *Nat Commun.* 2016;7:13041. <https://doi.org/10.1038/ncomms13041>
35. Zhu S, Lu J, Lin Z, Abuzeid AMI, Chen X, Zhuang T, et al. Anti-tumoral effect and action mechanism of exosomes derived from *Toxoplasma gondii*-infected dendritic cells in mice colorectal cancer. *Front Oncol.* 2022;12:870528. <https://doi.org/10.3389/fonc.2022.870528>
36. DeBerardinis RJ, Lum JJ, Hatzivassiliou G, Thompson CB. The biology of cancer: metabolic reprogramming fuels cell growth and proliferation. *Cell Metab.* 2008;7(1):11–20. <https://doi.org/10.1016/j.cmet.2007.10.002>
37. Lau CHE, Tredwell GD, Ellis JK, Lam EWF, Keun HC. Metabolomic characterisation of the effects of oncogenic PIK3CA

- transformation in a breast epithelial cell line. *Sci Rep.* 2017;7:46079. <https://doi.org/10.1038/srep46079>
38. Menendez JA, Vellon L, Mehmi I, Oza BP, Ropero S, Colomer R, et al. Inhibition of fatty acid synthase (FAS) suppresses HER2/neu (erbB-2) oncogene overexpression in cancer cells. *Proc Natl Acad Sci U S A.* 2004;101(29):10715–20. <https://doi.org/10.1073/pnas.0403390101>
39. Bao X, Shi R, Zhao T, Wang Y, Anastasov N, Rosemann M, et al. Integrated analysis of single-cell RNA-seq and bulk RNA-seq unravels tumour heterogeneity plus M2-like tumour-associated macrophage infiltration and aggressiveness in TNBC. *Cancer Immunol Immunother.* 2021;70(1):189–202. <https://doi.org/10.1007/s00262-020-02669-7>
40. Kaneda MM, Messer KS, Ralainirina N, Li H, Leem CJ, Gorjestani S, et al. PI3K γ is a molecular switch that controls immune suppression. *Nature.* 2016;539(7629):437–42. <https://doi.org/10.1038/nature19834>
41. De Henau O, Rausch M, Winkler D, Campesato LF, Liu C, Cymerman DH, et al. Overcoming resistance to checkpoint

blockade therapy by targeting PI3K γ in myeloid cells. *Nature.* 2016;539(7629):443–7. <https://doi.org/10.1038/nature20554>

SUPPORTING INFORMATION

Additional supporting information can be found online in the Supporting Information section at the end of this article.

How to cite this article: Han B, Han X, Luo H, Nasir J, Chen C, Shao Z, et al. Multiomics and single-cell sequencings reveal the specific biological characteristics of low Ki-67 triple-negative breast cancer. *Cancer Innov.* 2024;3:e146. <https://doi.org/10.1002/cai2.146>